Small Particle Collection by Supported Liquid Drops

YHUDA GOLDSHMID and SEYMOUR CALVERT

Case Institute of Technology, Cleveland, Ohio

The collection of small particles on liquid surfaces is encountered in gas-liquid contacting and gas-cleaning devices. The specific situation may range from the separation of relatively large drops of entrained liquid to mist removal and to the collection of small solid or liquid particles in the micron size range. Depending on the equipment design and the operating conditions the liquid phase may be continuous or discontinuous and supported by a solid structure or not.

A customary situation involves a discontinuous (or semicontinuous) liquid phase which flows down supporting packing. Studies of transfer processes in such systems have largely related to the case of thin films of liquid flowing down vertical or inclined surfaces. Very little attention has been given to the case of small bodies of liquid being held for a period of time on top of a supporting element. The striking increase in contacting efficiency in the region of the flooding point leads us to consider the mechanism of transfer to supported oscillating bodies as at least a partial explanation and, if so, as a phenomenon to be exploited.

This study deals with the collection of small particles by single drops supported on wires. Regions of operation in which the drop is held up and oscillated by the air stream and in which the major collection mechanism is inertial impaction are of interest.

BACKGROUND

The phenomenon of particle collection by objects of different shapes, has been the subject of many experimental and theoretical studies. Three different collection mechanisms, inertia, diffusion, and interception, have been postulated and proved. This study was limited to the collection by inertia mechanism only, thus very high air velocities and very low $(r_p)/(R_c)$ ratios were employed.

Theoretical solutions for the collection of particles by spheres and bodies of other geometries were developed by many (*36, 16, 23, 42, 10, 26, 31, 40, 25, 12, 38, 8*). All of them make several simplifying assumptions to be able to formulate and solve the problem. The main assumptions made are:

1. Each particle that hits the obstacle sticks to it.
2. For high Re numbers a potential flow and for low Re numbers a viscous flow are assumed.
3. Collection is on front of obstacle only.

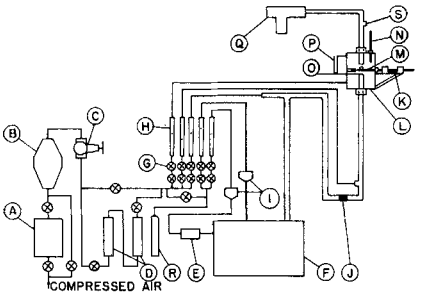

Fig. 1. Experimental setup.

The validity of these assumptions was discussed in the literature (*27, 43, 29*), and it seems that part of the experimental results contradict them (*28, 27*), while the other part agrees with one or another segment of the theoretical curves (*32, 43*).

The mathematical analysis yielded a set of dimensionless equations describing the path of the particle in the neighborhood of the obstacle. They have the form

$$K V_x \frac{dV_x}{dx} = \left(\frac{Cd\, N_{Re}}{24}\right)(V_x - U_x)$$

where

$$K = \left(\frac{2\rho_p U_o r_p^2}{9\mu R_c}\right) F$$

is the inertia parameter, V_x and U_x are dimensionless velocity components of the particle and the air in the x direction, and x is a dimensionless distance in the x direction. From the equation it is seen that two parameters are needed to describe the collection efficiency, K and $(Cd\, N_{Re}/24)$. Sherman, Klein, and Tribus (*37*) have shown that trajectories can be described with sufficient accuracy by choosing an appropriate average value of $(Cd\, N_{Re}/24)$ which is designated as λ/λ_s, the ratio of actual to Stoke's law stopping distances:

$$\frac{\lambda}{\lambda_s} = \frac{1}{(N_{Re})_{po}} \int_o^{(N_{Re})_{po}} \frac{24}{Cd\,(N_{Re})_p}\, d\,(N_{Re})_p$$

The values of Cd and N_{Re} are those determined empirically for solid spheres. Langmuir and Blodgett (*26*) defined a parameter $K_o = \lambda/\lambda_s K$. Thus one curve will describe the relationship between K_o and E.

Most of the experimental work was done on the collection of particles by a cylinder or arrays of cylinders (*9, 13, 17, 23, 30, 32, 33, 35, 44, 5, 6, 20*). The collection of sulfuric acid particles by a platinum sphere was measured by Ranz and Wong (*32*), and the only collection efficiency measurements using supported drops as the collectors were made by Walton and Woolcock (*43*) who employed methylene blue dust and water drops suspended on a glass capillary. Both studies gave results which agreed quite well with the theory used.

DROP MECHANICS

When high air velocities are employed in measuring the collection efficiency, and when drops are used as collectors, drop distortion and oscillation may increase collection efficiency,

Yhuda Goldshmid is with the American Standard Company, Union, New Jersey.

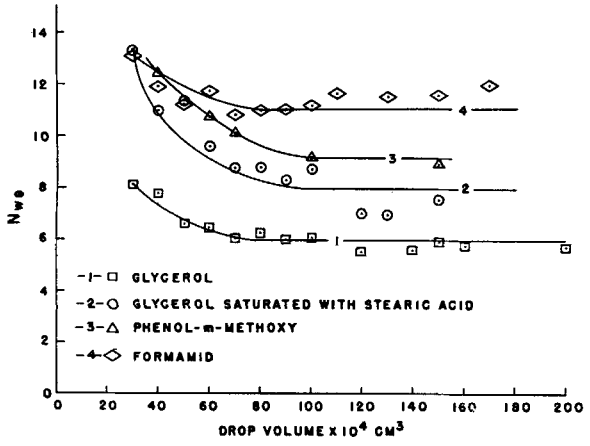

Fig. 2. Shattering of glycerol formamide and phenol-m-methoxy drops.

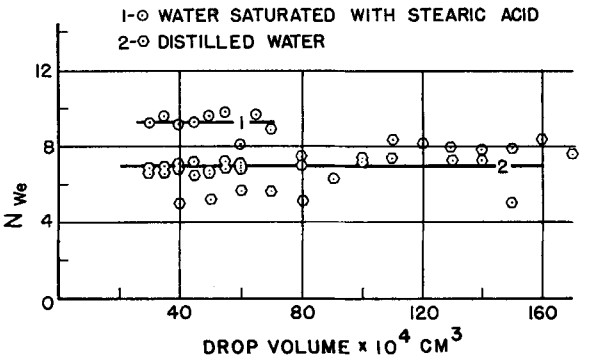

Fig. 3. Shattering of water drops.

while drop shattering will provide the higher limit for air velocity. The mechanics of supported drops can be described by the same groups used to describe unsupported drops as will be shown by the experiments conducted in this study and those conducted by Constan (7).

The distortion of drops are of two basic types: those of an equilibrium nature, and those of an oscillatory nature resulting from vibrations about this equilibrium position. Most of the investigators in this field (*11, 19, 34, 39*) reached the conclusion that a correlation should exist between the *We* group and the amount of distortion the drop suffers. Best (*2, 3*) and Finlay (*11*) showed that falling drops could best be approximated by two half-ellipsoids of revolution, with common major and differing minor axes. Finlay's work also showed that surface tension and liquid density, as well as drop size, play the major part in determining the drop shape. Liquids with both low viscosity and low surface tension give drops which behave abnormally in that they can no longer be described as ellipsoid because of unusual oscillations. Finlay (*11*) for unsupported and Constan (7) for supported drops show that for the range of drop sizes used in this study the change in the projected cross-sectional area, owing to distortion is less than 10%.

Observations on drops suspended in an upward air current (*4, 15*) have shown that deformation is accompanied by oscillation of the drop about its own axes. The oscillations have been variously reported as prolate oblate ellipsoidal changes; constant drop deformation in the horizontal plane accompanied by a rotation about the vertical axes; periodic oscillation about axes 90 deg. apart in the horizontal plane. In the case of supported drops, Constan (7) described in addition a fourth type of oscillation which he called a *displacement* and which consists of two types:

1. The drop remains attached to the support in the same place but its center of gravity moves along the axes of the support.
2. The shape of the drop remains the same while it wiggles, with the support as a hinge.

Constan (7) measured the amplitude of water drops supported by hypodermic tubing and found it to be in the order of 10% of drop diameter. He also measured supported drop oscillation frequencies, while Finlay (*11*) and Garner and Lane (*14*) measured frequencies of free drops. They all compared their results to the values calculated using Lamb's (*22*) equation

$$f = \left(\frac{8\sigma}{3\pi m}\right)^{1/2}$$

The agreement was quite good for the free drops as long as the oscillation was of the problate oblate ellipsoidal type. With the supported drops the agreement was not as good but still within an order of magnitude.

Free drop shattering was measured and described in several works (*21, 24, 41*). They all characterized drop shattering by a critical N_{We} number. Hinze (*18*) calculated $(N_{We})_{crit}$ for different liquids and found it to be between 7.7 and 15.0.

OBJECTIVES

The objectives of this study were to get a better understanding of the basic factors which influence the collection of small particles by supported drops and to supplement the meager amount of experimental information available regarding collection of particles by drops. This was done by studying the influence on the collection efficiency of supported drops of drop physical properties, drop size, drop oscillation, interfacial tension between the drop liquid and the aerosol, high air velocities, particle diameter, and particle physical properties.

EXPERIMENTAL

To determine the effects that the abovementioned factors have on the collection efficiency of particles by supported drops, different aerosols were produced, and the collection of these aerosols by supported drops was measured. The drops were supported on a horizontal hypodermic tubing by an upward-flowing air stream laden with the aerosol. The various drops used as collectors and the air stream were analyzed and the collection efficiency determined.

Equipment and Procedure

The experimental setup is shown in Figure 1. Air at 90 lb./sq. in. gauge sup-

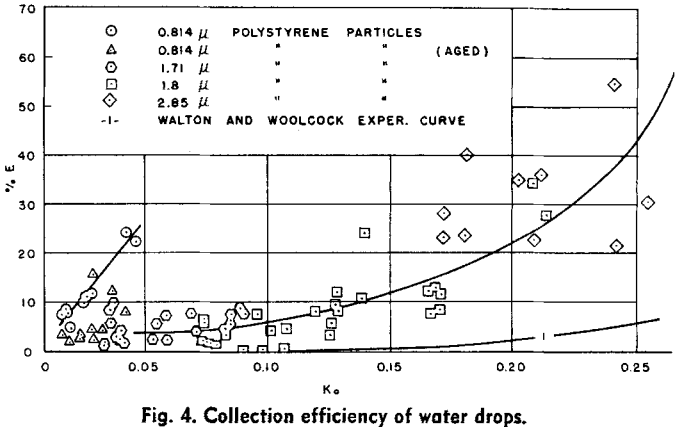

Fig. 4. Collection efficiency of water drops.

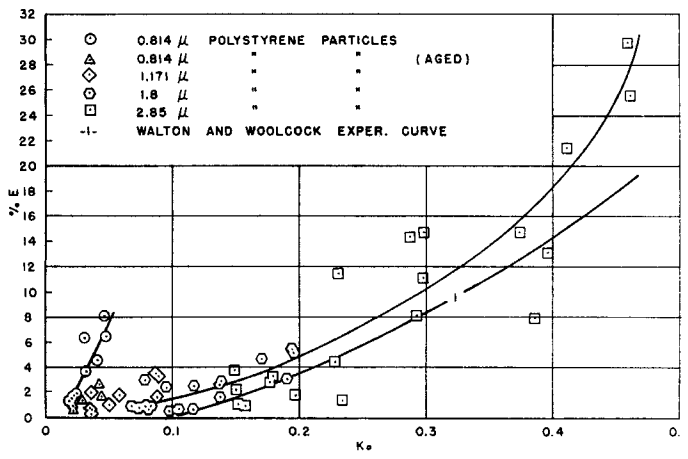

Fig. 5. Collection efficiency of glycerol drops.

plied by a two-stage compressor passed through a silica gel dryer, A, which reduced the relative humidity to below 1%, and then through a filter, B. The pressure was then reduced to 20 lb./sq. in. gauge by the pressure-regulating valve, C. When water drops were used as collectors the air bypassed the dryer and flowed instead through two packed humidifiers in series D. The dry or wet clean air flow was controlled by two needle valves, G, and measured by the rotameters, H. Air supplied to the LaMer-Sinclair type of aerosol generator F was refiltered by passing it through the membrane filters, I. When polystyrene spherical particles were used no refiltering was needed. The LaMer-Sinclair generator was heated for several hours, until a homogeneous spherical aerosol which possessed the desired average particle size was produced. The aerosol was diluted to give the predetermined air velocity ranging from 900 to 1,700 cm./sec. and the aerosol stream was then passed through the piece of tubing, J, to a $2 \times 4 \times 6$ in. plexiglass box serving as the working section, L. The drop was produced and measured by rotating the microburette handle, K, and was supported above a 22-gauge s.s. tubing, M, by the aerosol stream coming out of the nozzle, O. The velocity profile of the air stream emerging from the nozzle, O, was measured at different air velocities and found to be practically flat. Air was supplied through a side line so as to force all the aerosol out through the glass tubing connected to the electrostatic precipitator, Q. The aerosol was precipitated on an aluminum sheet inside the collecting tube of the precipitator. When the run ended, the drop was drawn away from the supporting tube to a syringe with a long needle, the electrostatic precipitator stopped and the tubing disconnected.

Analysis

When polystyrene latex was used the drop was diluted into a 1-cc. volumetric flask and the particles were counted under a microscope in a blood counting cell. The aluminum tube from the electrostatic precipitator was washed into a 100-cc. volumetric flask and the particles counted in a blood counting cell.

When using sulfur aerosol, produced by the LaMer-Sinclair generator, several drops were washed into a 50-cc. volumetric flask with 95% redistilled ethyl alcohol. The sample introduced into a 10-cm. silica cell, and the percentage of transmission measured at 275 mμ with a spectrophotometer; graphs which did not agree within 5% were discarded. The total amount of aerosol used was determined by weighing the aluminum foil which covers the electrostatic-precipitator collecting tube, before and after collection, on a semimicro analytical balance.

Particle size was determined by taking pictures of the aerosol deposited on a glass slide inside the electrostatic precipitator under the microscope (970x) in the two far sides of the deposited aerosol. The picture was magnified again using a microfilm reader so that $1\mu = 4$mm. (4,000x). The images were then measured with a ruler marked to 0.5mm. Contact angles were measured by taking a picture of a drop on a glass slide covered with the aerosol. This method was chosen to get the aerosol in the same condition as used during the experiments. The contact angle was calculated from the relationship

$$tg \frac{\alpha}{2} = \frac{h}{r} \quad (\alpha < 90)$$

given by Adamson (*1*), where h is the height of the drop above the surface and r is the radius of the circle the drop formed with the slide.

This treatment assumes a spherical shape for the drop and neglects gravitational effects. From the measured quantities collection efficiency was calculated according to the assumption that the drops are spherical and the concentration of particles over the flow cross-sectional area is a constant.

Collection efficiency was then plotted vs. the modified inertia parameter K_0 calculated from the known air velocity and physical properties of the air and aerosol.

Five liquids were used as drops during the experiments: water, glycerol, phenol-m-methoxy, formamide, and n-hexadecane. These drops were chosen because they all have high boiling points, so that no liquid will be lost through evaporation; all, except for n-hexadecane, possess high surface tensions to make them stable; and all dissolve in alcohol or water and do not disturb the measurements.

Two aerosols were used during the experiments, polystyrene and sulfur. The polystyrene was diluted, dispersed through a nebulizer, and dried. The sulfur aerosol was produced by the LeMer-Sinclair generator.

RESULTS

Shattering of Drops

Shattering of drops was measured by introducing a drop of known size above the supporting needle and gradually increasing air velocity until shattering was observed. The air velocity was then measured and the *We* group calculated after measuring drop-surface tension. Drop diameter was calculated from known drop volume assuming a spherical shape. The results for different liquids, or liquids saturated with stearic acid, are given in Figures 2 and 3 as N_{We} vs. drop volume.

These results show that supported drops behave in the same way as free drops, with respect to shattering, when larger than a certain volume. Above a critical N_{We} number which does not change with drop dimension drops will shatter. Drops smaller than the above-mentioned volume show a higher critical N_{We} number. It seems in the case of the smaller drops that the needle

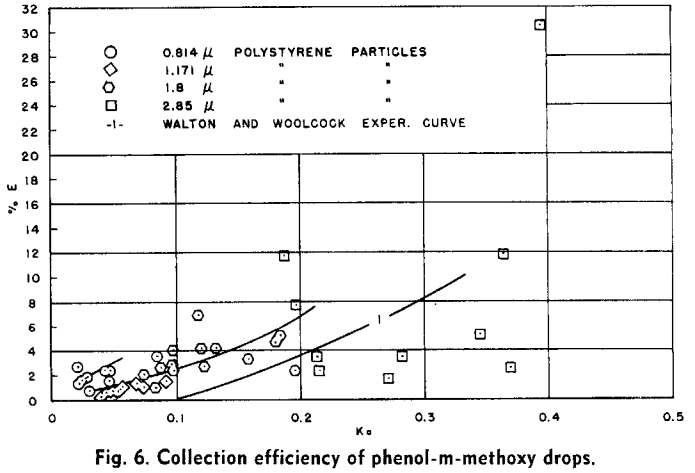

Fig. 6. Collection efficiency of phenol-m-methoxy drops.

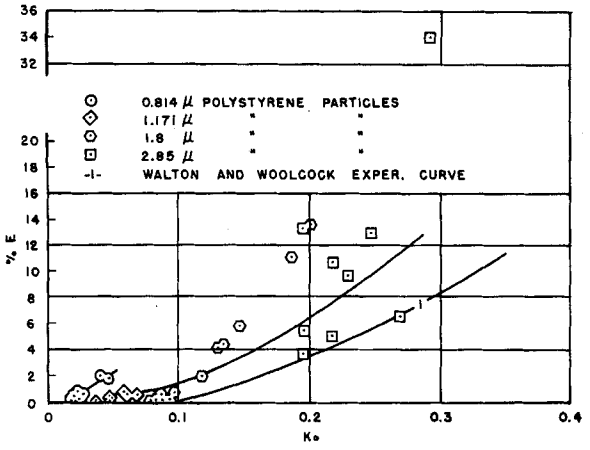

Fig. 7. Collection efficiency of formamide drops.

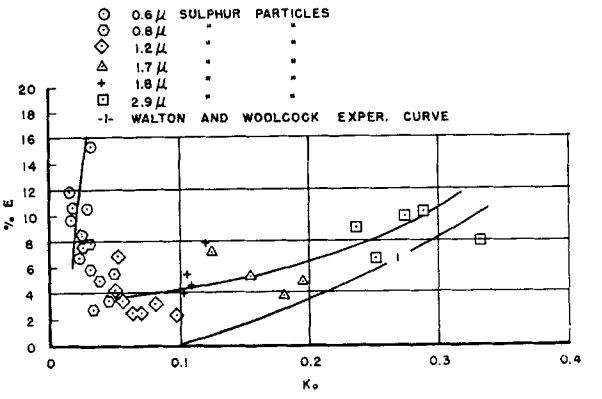

Fig. 8. Collection efficiency of n-hexadecane drops.

protects the drop and a higher air velocity is needed to cause shattering.

During the shattering experiments, it was observed that drops do not get torn away from the supporting needle, but that the drop itself shatters. This observation lends support to the conclusion that both supported and free drops behave in the same way when shattering.

Collection of Polystyrene Aerosol by Supported Drops

The collection efficiency of different size aerosol particles by supported drops was measured and calculated as described. The results are plotted in Figures 4 through 7 as collection efficiency of polystyrene particles of different diameters by one liquid vs. the modified inertia parameter. Points measured, using different size particles, are drawn in different ways. The data are compared, where possible, with Walton and Woolcock's (43) experimental curve for the collection of methylene blue particles by water drops. (Walton and Woolcock data were taken at lower air velocities.)

All the figures took the expected shape as calculated by Langmuir and Blodgett (26) or Fonda and Herne (12). It should be noticed here that curves for 2.85μ polystyrene particles show very high scattering of experimental results. This resulted from the aerosol of 2.85μ particles being too dilute. Thus, the number of particles counted was not enough to give a statistical certainty.

Collection of Sulphur Aerosols by Supported Drops

The results were again plotted in the same way as before so as to get the general shape of the curves and the influence of drop material on collection efficiency.

Figures 8, 9, and 10 are plots of collection efficiency vs. modified inertia parameter. Each curve describes the collection efficiency of one liquid and is compared to Walton and Woolcock experimental curves.

Effect of Oscillation on Collection Efficiency

The effect of oscillation on collection efficiency was determined by measuring the collection efficiency of stationary and oscillating glass spheres. In this way all other effects, such as surface effects, were eliminated. No difference was found between the collection efficiency of the two, when air velocities of 0.75 to 1.25 times the oscillating velocities were employed.

DISCUSSION

Effect of Interfacial Tension of Collection Efficiency

A difference was observed visually in the mutual behavior of aerosol-drop pairs depending upon whether they wet or do not wet each other. When the drop was left exposed to the aerosol stream for relatively long periods of time, 5 to 10 min., an aerosol crust was formed around the drop. This crust stopped drop oscillation and, when the air stream was stopped, kept the drop above the support against the gravitational forces. These effects were never observed with pairs that wet each other. In addition, the experimental results showed that mutually nonwetting pairs gave lower collection efficiencies than the mutually wetting pairs for the same inertia parameter.

Figure 11 shows the collection efficiency vs. *Ko* with contact angle between the aerosol and drop as parameter. The pairs, polystyrene-glycerol, polystyrene-formamide, and *n*-hexadecane-sulfur, show the same collection efficiency within experimental error. The pair, polystyrene-water, shows a higher collection efficiency. The reason

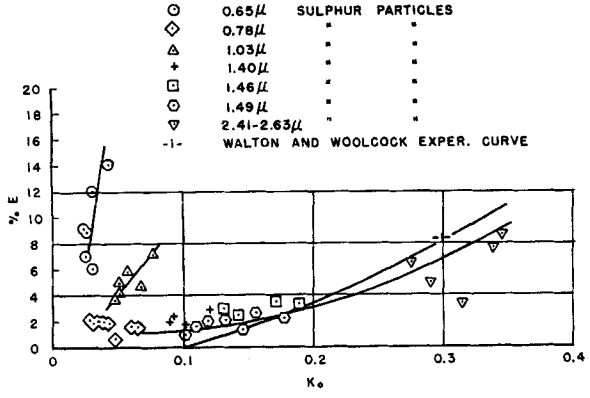

Fig. 9. Collection efficiency of water drops.

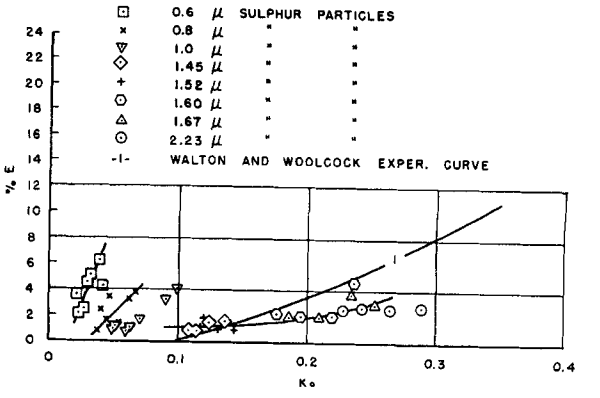

Fig. 10. Collection efficiency of glycerol drops.

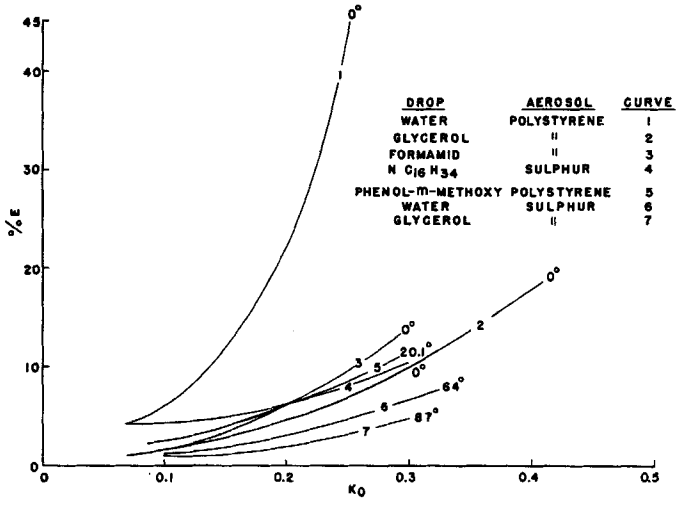

Fig. 11. Collection efficiency of drops with contact angle as parameter.

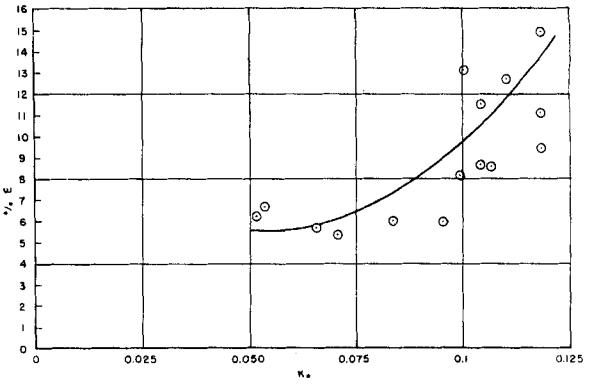

Fig. 13. Collection efficiency of glass spheres at high air velocities.

may be the surface active agent present in the polystyrene solution which seems to cover each polystyrene particle in a very thin layer. The effect of interfacial tension on the collection efficiency can be observed from the behavior of the other three pairs. The collection efficiency seems to drop with the increase in contact angle or with the decrease of mutual wetting. This figure shows a definite effect of interfacial tension on the collection efficiency.

Some writers (2) tried to overcome the difficulty in measuring the interfacial tension by saying that the collection efficiency decreases with increase in surface tension, other parameters being the same. This does not seem to be the case since water has a higher surface tension than glycerol, yet it shows higher collection efficiencies.

A New Mechanism for the Collection of Small Particles at High Air Velocities

An interesting feature of the collection-efficiency curves for all the drops used, is the sudden increase in collection efficiency for very small particles ($D < 1\ \mu$) at the particularly high air velocities employed in this study. None of the mechanisms suggested up to now and described previously predicts such an effect, or is able to explain it. The inertia mechanism predicts a monotonic decreasing curve for decreasing K, and, as explained before, the experimental conditions were chosen so as to make the effect of the diffusion and interception mechanisms negligible. It is interesting to note that Ranz and Wong (32), working with even smaller particles and lower stream velocities, reported no such behavior.

It was suggested that the increase in collection efficiency is due to inertial collection of particles by the back of the sphere. The experimental evidence concerning flow past a sphere describes the flow in the back of the sphere as a shedding vortex loop in the range of N_{Re} of 1,000 to 8,000 (42) which includes the range of N_{Re} used here. It was assumed then, that the curved streamlines act on the particles so as to make them change their original course and follow the streamlines. The larger particles which possess a high momentum do not do so, while the smaller ones follow the streamlines and are thrown out of the vortex on the back of the collector by the centrifugal force.

This effect could have been calculated in the same manner as the inertial mechanism for the front of the sphere were the flow-line pattern in the back of the sphere available. Since the literature survey showed that no analytical description of such flow patterns is available for the range of N_{Re} employed in these experiments, it was decided to try a very simplified analysis as a basis for a quantitative estimate of the magnitude of such a mechanism in order to assess its plausibility.

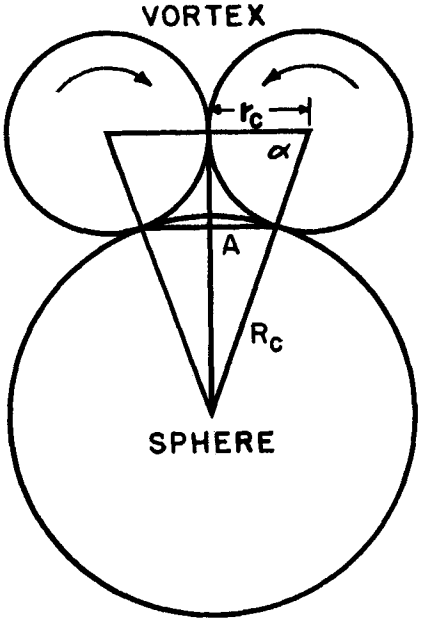

Fig. 12. Collection by the back of a sphere.

The following assumptions were made:

1. The concentration of particles in the vortex ring is the same as in the main stream (very rapid transfer of particles into the vortex).
2. The diameter of the vortex ring is half the diameter of the sphere (Figure 12).
3. The tangential velocity of the vortex is the same as the main stream velocity.
4. The particles obey Stoke's law.
5. Every particle which hits the sphere sticks to it.
6. Particles start to be deposited only after passing the central tangent point of the two parts of the vortex. (Deposition occurs over an angle α. See Figure 12.)

The terminal settling velocity U_t of a particle obeying Stoke's law in a gravitational field is given by Equation (1):

$$U_t = \left(\frac{d_p^2 g \rho_p}{18\mu}\right) F \qquad (1)$$

The radial settling velocity U_r of a particle in a centrifugal field, at any distance r_c from the center of the vortex and having a tangential velocity $U = U_o$ is given by Equation (2):

$$U_r = U_t\left(\frac{a_c}{g}\right) \qquad (2)$$

The centrifugal acceleration a_c is

$$a_c = \frac{U^2}{r_c} \qquad (3)$$

In accordance with the sixth assumption above, the time in which deposition occurs is given by Equation (4):

$$t = \left(\frac{\alpha}{360}\right)\frac{2\pi r_c}{U_o} \qquad (4)$$

The distance β a particle will travel in the radial direction in time t is

$$\beta = U_r t = \left(\frac{\alpha\pi}{180}\right)\left(\frac{U_o U_t}{g}\right) \qquad (5)$$

From Figure 12 $\cos \alpha = 1/3$ and $\frac{\alpha}{180} = 0.392$. The total volume of gas cleaned per unit time is

$$V_c = \pi A \beta U_o \qquad (6)$$

where

$$A = \frac{2 R_c}{3}$$

according to the sixth assumption mentioned above. Using the definition of the collection efficiency

$$E = \frac{V_c}{U_o \pi R_c^2} \qquad (7)$$

and substituting Equations (1), (5), (6) into Equation (7) one obtains

$$E = 0.823 K = BK$$

This equation agrees with the experimental data, since straight lines were found to describe the collection efficiency vs. K for small particle sizes. The analysis did not consider the forces moving the particles from the main stream to the vortex. As a result, B came out to be a constant. Actually, B should be a certain function of $\left(\frac{1}{d_p}\right)^q$.

Diameter Limit

Another interesting result followed from calculating the smallest particle that will be cast out of the vortex before even getting into the area confined by the angle α. With Equation (5) and experimental data used it followed that even if the 1 μ particles will follow the stream lines and enter the vortex loop, they will be thrown out of it. This means that particles larger than 1 μ could not be caught on the back of drops (of sizes used in these experiments) by the back collection mechanism which again agrees with the experimental results.

To check the validity of this assumption, two experiments were run. In the first, a glass sphere was exposed to the aerosol stream for 10 to 15 min. and then viewed under the microscope. The microscopic examination showed a layer of particles on the back and practically nothing on the front of the collecting sphere.

In the second experiment, collection efficiency was determined for glass spheres using sulfur particles of 0.8 μ and employing very high air velocities up to about 4,700 cm./sec. It was predicted that a straight line should exist at low K values corresponding to the inertia collection mechanism. When the back collection mechanism takes over, a sharp increase in the slope of the curve should occur with a magnitude much higher than what can be expected from the front-face inertia mechanism. The experiment was carried out and the results are plotted in Figure 13. It is seen that the curve behaved as predicted, showing a collection efficiency of 15% for $K = 0.118$ while Langmuir and Blodgett predict only about 2% for the same K value.

Comparison of the Experimental Curves to Walton and Woolcock Experimental Data

In all cases, the curves for the collection efficiency seem to be above the one obtained by Walton and Woolcock for pendant drops. Two factors may contribute to this increase in collection efficiency, and both are connected to the drop's shape.

The collection efficiency was calculated on the basis of the drops being spherical, but the distorted drops take the shape of an ellipsoid of revolution, as indicated previously, which has a larger cross-section. The second factor is also concerned with the shape of the collector. The collection efficiency for a disk, as calculated by Ranz and Wong (*15, 16*), is higher than the one for a sphere and the shape of the distorted drop is between a sphere and a disk. Thus, both these effects tend to increase the collection efficiency above the one for undistorted spheres.

CONCLUSION

The following conclusions have been reached:

1. Supported drops behave with respect to shattering in the same manner as free drops when they are larger than a critical size. This, with the measurements made by Constan (7) regarding a drop's oscillation period and amplitude, shows that supported drops behave in the same manner as free drops.

2. Collection efficiency was measured in the designated region and plotted vs. a modified inertia parameter K_o. Collection efficiency curves take the same shape as predicted by theory.

3. Oscillation does not affect the collection efficiency, and drop distortion has a slight effect on collection efficiency, owing to change of shape and increase in cross-sectional area.

4. The effect of interfacial tension is a predominant one. Drops that wet particles show better collection efficiency than those which do not wet, and the higher the contact angle the lower the collection efficiency.

5. A new mechanism, inertia collection by the back of the drop at high air velocities and small particle sizes ($d_p < 1$ μ), was postulated and proven experimentally. This mechanism may increase the collection efficiency from practically zero to over 20% in the region of particle sizes where dust collection efficiencies are very low.

ACKNOWLEDGMENT

This investigation was supported in large part by Research Grant S-84 from the Division of Sanitary Engineering Services, U.S. Public Health Service.

NOTATION

a_c = centrifugal acceleration cm./sec.^{2}
B = constant, dimensionless
Cd = drag coefficient, dimensionless
d_p = particle diameter, cm.
E = collection efficiency, percent
f = frequency of oscillation, sec.$^{-1}$
F = Cunningham slip correction factor
q = acceleration of gravity, 981 cm./sec.^{2}
K = inertial collection parameter, dimensionless
K_o = modified inertial collection parameter, dimensionless
m = drop mass, g.
r_c = vortex radius, cm.
r_p = particle radius, cm.
R_c = collector radius, cm.
$(N_{Re})_p$ = Reynolds number $d_p U \rho / \mu$
$(N_{Re})_{po}$ = Reynolds number based on undisturbed gas velocity $d_p U_o \rho / \mu$
t = time, sec.
U = particle velocity relative to the gas, cm./sec.
U_o = undisturbed gas velocity, cm./sec.
U_r = radial velocity of particle, cm./sec.
U_t = terminal velocity of particle cm./sec.
U_x = dimensionless air velocity in the x direction U_x/U_o
U_x = air velocity component in the x direction cm./sec.
V_x = dimensionless particle velocity in the x direction v_x/U_o
v_x = particle velocity component in the x direction cm./sec.
V_c = volume of gas cleaned per unit time cc./sec.
N_{We} = Weber group $\rho_g U^2 R_c/\sigma$
X = dimensionless distance in the x direction x/R_c
x = distance along x coordinate, cm.

Greek Letters

α = contact angle
μ = air viscosity g./cm. sec.
λ/λ_s = the ratio of the distance a particle will travel if projected into still air with velocity U_o, to the range it would have if the drag force were that of Stoke's
ρ_p = particle density, g./cc.
σ = surface tension, dynes/cm.

LITERATURE CITED

1. Adamson, A. W., "Physical Chemistry of Surfaces," Interscience, p. 270, New York (1960).
2. Best, A. C., Great Britain Air Ministry Meteorological Committee, 330/1947.
3. *Ibid.*, 277/1946.
4. Blanchard, D. G., *Trans. Am. Geophys. Union*, **31**, 836, (1950).
5. Brink, J. A., *Proc. Air Water Pollution Abatement Conf.*, p. 104 (1959).
6. Chen, C. Y., *Chem. Revs.*, **55**, 595 (1955).
7. Constan, G. L., Ph.D. thesis, Case Inst. Technol., Cleveland, Ohio (1961).
8. Das, P. K., *Indian J. Meteorol. Geophys.*, **1**, 137 (1950).
9. Davis, C. N., *Proc. Inst. Mech. Engrs. (London)*, B **1B**, 185 (1952).
10. Dorsch, R. G., P. G. Saper, and C. F. Kadow, *Nat'l. Advisory Comm. Aeronaut. Tech. Note 3587* (1955).
11. Finlay, B. A., Ph.D. thesis, Univ. Birmingham, Edgbaston, England (1957).
12. Fonda, A., and H. Herne, National Coal Board (Great Britain) Mining Research Establishment Report *No. 2068* (1957).
13. Gallily, Isaiah, *J. Colloid Sci.*, **12**, 161 (1957).
14. Garner, F. H., and J. J. Lane, *Trans. Inst. Chem. Engrs. (London)*, **37**, 162 (1959).
15. General Electric Research Laboratory Report *R.L. 140* (1950).
16. Glauert, Herman, Aeronautical Research Committee Report *No. 2025 (London H.M.S.O.)* (1940).
17. Gregory, P. H., *Ann. Appl. Biol.*, **38**, 357 (1951).
18. Hinze, J. O., *Appl. Sci. Research*, **A1**, 273 (1948).
19. ———, *A.I.Ch.E. Journal*, **1**, 289 (1956).
20. Jarman, R. T., *Chem. Eng. Sci.*, **10**, 268 (1959).
21. Klüsener, O. Z., *Ver. deut. ing*, **77**, 171 (1933).
22. Lamb, Horace L., "Hydrodynamics," 6 ed., Cambridge Univ. Press, London, England (1932).
23. Landahl, H. D., and R. G. Herman, *J. Colloid Sci.*, **4**, 103 (1949).
24. Lane, W. R., *Ind. Eng. Chem.*, **43**, 1312 (1951).
25. Langmuir, Irving, *Met.*, **5**, 175 (1948).
26. ———, and K. B. Blodgett, *Army Air Force Techn. Rept. 5418* (1946).
27. McCully, C. R., M. Fisher, G. Langer, J. Rosinski, H. Glaass, and D. Werle, *Ind. Eng. Chem.*, **48**, 1512 (1956).
28. Oakes, Billy Dean, *Intern. J. Air Pollution*, **3**, 179 (1960).
29. Pemberton, C. S., *ibid.*, 168.
30. Ramskill, E. A., and W. L. Anderson, *J. Colloid Sci.*, **6**, 416 (1951).
31. Ranz, W. E., *Dept. of Eng. Research Rept. No. 66*, Penn. State Univ., State College, Pennsylvania (1956).
32. ———, and J. B. Wong, *Ind. Eng. Chem.*, **44**, 1371 (1952).
33. Ranz, W. E., and J. B. Wong, *A.M.A. Arch. Ind. Hyg. Occupational Med.*, **5**, 464 (1952).
34. Savic, Pavle, *Nat'l. Research Council of Canada Report. No. MT-22* (1953).
35. Schadt, Conrad, and R. D. Cadle, *Anal. Chem.*, **29**, 864 (1957).
36. Sell, W., *VDI Forschungsheft No. 347* (1931).
37. Sherman, Pauline, J. Klein, and M. Tribus, *Eng. Research Inst. Technical Rept.*, Univ. Mich., Ann Arbor, Michigan.
38. Stairmand, E. J., *Trans. Inst. Chem. Engrs. (London)*, **28**, 130 (1950).
39. Taylor, G., Ministry of Supply (Chem. Defense Experimental Station) Proton, England, 6600/5278/49.
40. Taylor, G. I., *Aeronautical Research Commission Reports and Memoranda 2024*, London, England (1940).
41. Tribnigg, A., "Der Einblase and Einspritzvorgang bei Dieselmaschinen," Vienna, Austria (1929).
42. Torobin, L. B., and W. H. Gauvin, *Can. J. Chem. Eng.*, **37**, 167 (1959).
43. Vasseur, Marcell, *Res. Aeronaut.*, **9**, 1 (1949).
44. Walton, William H. and Allan Woolcock, *Intern. J. Air Pollution*, 3, 129 (1960).
45. Wong, J. B., W. E. Ranz, and H. F. Johnstone, *J. Appl. Phy.*, **26**, 244 (1955).

Manuscript received April 1, 1962; revision received September 24, 1962; paper accepted October 30, 1962. Paper presented at A.I.Ch.E. Los Angeles meeting.

Total and Form Drag Friction Factors for the Turbulent Flow of Air Through Packed and Distended Beds of Spheres

CHARLES A. WENTZ, JR., and GEORGE THODOS

Northwestern University, Evanston, Illinois

Several attempts have been made to determine the form and shear drag contributions to the overall friction factors for the flow of gases past spherical surfaces. Fage (4) has measured the static pressure around a single sphere 6 in. in diam. mounted in an open jet tunnel. His results indicate that the form drag caused by the static pressure on the surface of the sphere is the major component of the total drag, and that the contribution due to shear drag resulting from skin friction is relatively small. Similarly, Yen and Thodos (8) have determined, with a sensitive micromanometer, static-pressure profiles for the flow of air past a single celite sphere, 2.02 in. in diam. In his study, the total drag was also determined by measuring with an analytical balance the force exerted by air flowing past the sphere. Again, the results of this study indicate that the friction factors for total drag and for form drag resulting from the turbulent flow of air are of approximately the same order of magnitude. Flachsbart (3) has measured the pressure distribution around a single sphere for turbulent and nonturbulent conditions.

Although many investigators have measured the total pressure drop resulting from the flow of gases through packed beds of spherical particles (1, 2, 5), no attempts were made to resolve the resulting friction factors into their form-drag and shear-drag components. Therefore, in this study an effort has been made to account for the form and shear-drag contributions to the total drag for fixed beds by measuring the static pressure around the surfaces of test spheres contained in packed and distended beds of smooth plastic spheres.